

## Orbital Symmetry as a Tool for Understanding the Bonding in Krossing's Cation

Dirk V. Deubel<sup>1</sup>

Contribution from the Swiss Center for Scientific Computing, CSCS, Swiss Federal Institute of Technology, ETH Zürich, CH-6928 Manno, Switzerland, Academia Sinica, Institute of Biomedical Sciences, Taipei, Taiwan 11529, R.O.C., and University of Calgary, Calgary, Alberta, Canada T2N 1N4

Received May 7, 2002

**Abstract:** The geometric and electronic structure of Krossing's cation,  $\text{Ag}(\eta^2\text{-P}_4)_2^+$ , which shows an unexpected planar coordination environment at the metal center and  $D_{2h}$  symmetry both in solution and in the solid state, have been investigated using density functional theory and orbital-symmetry-based energy decomposition. The analysis reveals that the contribution from electrostatic interactions to the bond energy is greater than that of orbital interactions. Partitioning of the latter term into the irreducible representations shows that, in addition to the 5s orbital, 5p orbitals of silver act as acceptor orbitals for electron donation from  $\sigma(\text{P}-\text{P})$  orbitals ( $a_{1g}$ ,  $b_{1u}$ ) and  $n(\text{P})$  orbitals ( $b_{3u}$ ). Back-donation from the  $4d^{10}$  closed shell of Ag into  $\sigma^*$  orbitals of the pnictogen cages ( $b_{2g}$ ) is also important. However, this contribution is shown not to determine the  $D_{2h}$  structure, contradicting conclusions from the pioneering study of the title cation (*J. Am. Chem. Soc.* **2001**, *123*, 4603). The contributions from the irreducible representations to the stabilizing orbital interactions in the  $D_{2h}$  structure and in its  $D_{2d}$ -symmetric conformer are analogous, indicating that the planar coordination environment at the metal center in  $\text{Ag}(\eta^2\text{-P}_4)_2^+$  is induced by intermolecular rather than by intramolecular interactions. Because ethylene coordination to a metal ion is an elementary reaction step in industrial processes, the bonding in  $\text{Ag}(\text{C}_2\text{H}_4)_2^+$  has been analyzed as well and compared to that in Krossing's cation. Surprisingly, similar contributions to the bond energies and an involvement of metal 4d and 5p orbitals have been found, whereas a recent atoms in molecules analysis suggested that the metal–ligand interactions in silver(I) olefin complexes fundamentally differ from those in *tetrahedro*  $\text{P}_4$  complexes. The only qualitative difference between the bonding patterns in  $\text{Ag}(\eta^2\text{-P}_4)_2^+$  and  $\text{Ag}(\text{C}_2\text{H}_4)_2^+$  is the negligible energy contribution from the  $b_{3u}$  irreducible representation in the ethylene complex because a respective symmetry-adapted linear combination of ligand orbitals is not available.

### Objective

The first species with  $\eta^2$ -coordinated tetrahedral  $\text{P}_4$ ,  $\text{Ag}(\eta^2\text{-P}_4)_2^+$  (**1**), was recently reported by Krossing,<sup>2</sup> who succeeded in the synthesis of this fascinating compound by using large spectator anions containing an inert, perfluorinated surface.<sup>3</sup> Raman spectroscopy and single-crystal X-ray crystallography studies<sup>4</sup> revealed the unexpected  $D_{2h}$  symmetry of **1** with a planar coordination environment at the metal center (Figure 1).<sup>2</sup> It becomes clear that understanding the metal–ligand bonding in the spectacular molecule requires concepts different from those provided by traditional coordination chemistry. Density functional calculations of **1** were also presented<sup>2</sup> and a frontier-orbital analysis indicated an interaction of the occupied metal  $4d_{xz}$  orbital<sup>5</sup> with the  $\sigma^*$  orbitals of the P–P bonds (Figure 2). It was suggested<sup>2</sup> that the planar ligand field in **1** increases both the energy level of the  $d_{xz}$  orbital and the ability of the metal to

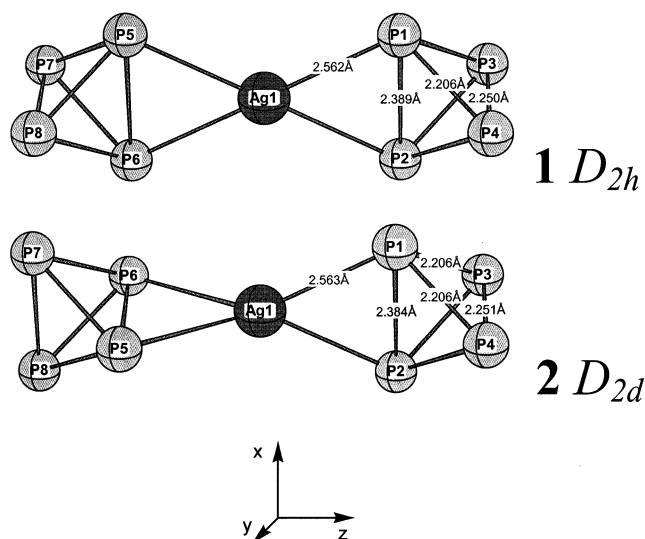


**Figure 1.** Calculated geometry (BLYP/V) of the conformers **1** and **2** of  $\text{Ag}(\eta^2\text{-P}_4)_2^+$ .

interact with vacant orbitals of the pnictogen cages. This interaction involving the  $4d^{10}$  closed shell of silver was

(1) URL: <http://staff-www.uni-marburg.de/~deubel>.

(2) Krossing, I. *J. Am. Chem. Soc.* **2001**, *123*, 4603.

(3) Krossing, I. *Chem. Eur. J.* **2001**, *7*, 490.

(4) Two solid-state structures of **1** were reported. The low-temperature modification (150 K) shows  $\text{Ag}(\eta^2\text{-P}_4)_2^+$  molecules with a slightly distorted  $D_{2h}$  symmetry and weak P–F contacts, while the 200 K structure shows  $D_{2h}$ -symmetric  $\text{Ag}(\eta^2\text{-P}_4)_2^+$  cations with the counterions freely rotating; for details, see refs 2 and 6.

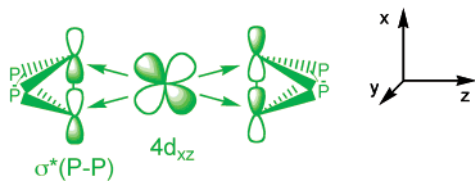


**Figure 2.** Is a specific  $d^{10}$ – $\sigma^*$  interaction the origin of the  $D_{2h}$ -symmetric structure of  $\text{Ag}(\text{P}_4)_2^+$ ?

proposed<sup>2</sup> to be considerably weaker in the  $D_{2d}$ -symmetric counterpart **2** with an approximately tetrahedral ligand field.

Heteroleptic and dinuclear derivatives of the title cation were recently synthesized<sup>6</sup> and other main-group-element complexes of silver(I) were reported.<sup>7</sup> The species were further characterized using a variety of experimental and computational techniques.<sup>6</sup> In particular, Krossing and van Wüllen<sup>6</sup> convincingly demonstrated that  $\text{Ag}(\text{P}_4)_2^+$  is the first species with  $\text{P}_4$  coordinating in an  $\eta^2$  fashion, while  $[\text{RhCl}(\text{P}_4)(\text{PPh}_3)_2]$ <sup>8</sup> should be considered a Rh(III) complex of the tetraphosahabicyclobutane dianion rather than a  $\text{P}_4$  complex of Rh(I). An atoms in molecules (AIM)<sup>9</sup> analysis of  $\text{Ag}(\text{P}_4)_2^+$  again indicates the activity of the  $4d^{10}$  shell, whereas a comparison with the AIM results of ethylenesilver(I) suggests a fundamentally different bonding and a predominance of electrostatic interactions in the ethylene complex.<sup>6,10</sup>

To understand the metal–ligand interactions in the title cation, we have studied silver(I) complexes using density functional theory (DFT), ab initio methods, and the energy-decomposition scheme introduced by Ziegler and Rauk.<sup>11–13</sup> This work focuses on the following goals: (i) Use of the high symmetry of  $\text{Ag}(\text{P}_4)_2^+$  to determine the contributions from the orbital interactions involving metal  $4d$ ,  $5s$ , and  $5p$  orbitals to the bond energy. The question whether  $np$  orbitals are valence orbitals of transition metals has been discussed controversially.<sup>13–16</sup> (ii)

Clarification of the stereoelectronic consequence of a potential  $4d_{xz}$ -orbital involvement, because the intramolecular induction of the unexpected  $D_{2h}$ -symmetric structure was recently postulated.<sup>2,6</sup> (iii) Comparison of the metal–ligand interactions in the title cation with those in  $\text{Ag}(\text{C}_2\text{H}_4)_2^+$ ; in particular investigation of the interplay of electrostatics and orbital interactions on one hand and by the determination of the contributions from the symmetry orbitals to the bond energy on the other hand. Do  $\eta^2 \text{P}_4$  and ethylene really show fundamentally different bonding patterns in their metal complexes, as suggested by the atoms in molecules results?

### Nature of the Bonding in $\text{Ag}(\text{P}_4)_2^+$

The molecular geometry of  $\text{Ag}(\text{P}_4)_2^+$  ( $D_{2h}$ , **1**) calculated at the BLYP level<sup>17,18</sup> using very large basis sets within the scalar-relativistic ZORA approximation<sup>19</sup> is presented in Figure 1 and Table 1. This is the theory level among those implemented in the ADF program<sup>20</sup> which gives the closest agreement between the calculated structure and a recently reported X-ray structure.<sup>6</sup> DFT-Hartree–Fock hybrid methods particularly improve the calculated distance between the metal-bound phosphorus atoms toward the experimental value (Table 1); for a comparison of the structures and energies of the title compounds at various levels of theory, see Supporting Information. Loss of translational and rotational entropy upon the formally trimolecular condensation,  $\text{Ag}^+ + 2 \text{P}_4 \rightarrow \text{Ag}(\text{P}_4)_2^+$ , partly compensates for the large bond enthalpies (Table 2).

The nature of the  $\text{Ag}$ – $\text{P}_4$  bond in the highly symmetric structure **1** has also been explored at the BLYP level using Ziegler and Rauk's<sup>11–13</sup> energy decomposition scheme. The results are presented in Table 3 and Figure 4. The analysis shows that the deformation of the equilibrium geometry of  $\text{P}_4$  toward its geometry in the complex requires a strain energy  $\Delta E_{\text{str}}$  of 8.3 kcal/mol, or 4.2 kcal/mol for each tetrahedron (Table 3). The energy of interaction  $\Delta E_{\text{int}}$  between the deformed phosphorus cages and the metal ion can be partitioned into three contributions ( $\Delta E_{\text{int}} = \Delta E_{\text{Pauli}} + \Delta E_{\text{elst}} + \Delta E_{\text{orb}}$ ). The repulsion of metal ion and ligands from each other because of the Pauli principle  $\Delta E_{\text{Pauli}}$  (148.3 kcal/mol), the electrostatic contribution  $\Delta E_{\text{elst}}$  (–127.1 kcal/mol), and the stabilizing orbital interactions  $\Delta E_{\text{orb}}$  (–115.9 kcal/mol) result in a total interaction energy of –94.7 kcal/mol and in a bond energy  $\Delta E$  of –86.4 kcal/mol ( $\Delta E = \Delta E_{\text{str}} + \Delta E_{\text{int}}$ ), or –43.2 kcal/mol for each  $\text{Ag}$ – $\text{P}_4$  bond (Table 3). The electrostatic stabilization  $\Delta E_{\text{elst}}$  is more important than the stabilization by orbital interactions  $\Delta E_{\text{orb}}$ .

The partitioning of the stabilizing orbital interaction  $\Delta E_{\text{orb}}$  into the contributions from the irreducible representations of the  $D_{2h}$ -symmetric complex is of particular interest. The molecular orbital (MO) diagram is presented in Figure 3 and the four main contributions to  $\Delta E_{\text{orb}}$  are displayed in Figure 4. The largest contribution arises from donation from the  $\sigma$  orbitals of the  $\text{P}$ – $\text{P}$  bonds into the vacant  $5s$  orbital of  $\text{Ag}$  ( $a_{1g}$ , –56.9 kcal/mol).<sup>21</sup> However, the interaction of  $\sigma(\text{P}–\text{P})$  with  $5p_z$  ( $b_{1u}$ ,

- (5) We have systematically used the group theoretical standard orientation of the axes in  $D_{2h}$  and  $D_{2d}$  symmetry as shown in the Figures. Cotton, F. A. *Chemical Applications of Group Theory*, 3rd edition; Wiley: New York, 1990.
- (6) Krossing, I.; van Wüllen, L. *Chem. Eur. J.* **2002**, *8*, 700.
- (7) (a) Krossing, I.; Raabe, I. *Angew. Chem., Int. Ed.* **2001**, *40*, 4406. (b) Krossing, I. *J. Chem. Soc., Dalton Trans.* **2002**, 500. (c) Adolf, A.; Gonsior, M.; Krossing, I. *J. Am. Chem. Soc.* **2002**, *124*, 7111.
- (8) (a) Ginsberg, A. P.; Lindsell, W. F.; McCullough, K. J.; Sprinkle, C. R.; Welsh, A. J. *J. Am. Chem. Soc.* **1986**, *108*, 403. (b) Göer, T.; Baum, G.; Scheer, M. *Organometallics* **1998**, *17*, 5916.
- (9) Bader, R. F. W. *Atoms in Molecules*; Clarendon Press: Oxford, England, 1994.
- (10) Hertwig, R. H.; Koch, W.; Schröder, D.; Schwarz, H.; Hrusák, J.; Schwerdtfeger, P. *J. Phys. Chem.* **1996**, *100*, 12253.
- (11) (a) Ziegler, T.; Rauk, A. *Theor. Chim. Acta* **1977**, *46*, 1. (b) Ziegler, T.; Rauk, A. *Inorg. Chem.* **1979**, *18*, 1755.
- (12) Decomposition schemes have proved to be valuable tools for an understanding of the chemical bond and reactivity; for recent examples, see: (a) Deubel, D. V.; Frenking, G. *J. Am. Chem. Soc.* **1999**, *121*, 2021. (b) Macdonald, C. L. B.; Cowley, A. H. *J. Am. Chem. Soc.* **1999**, *121*, 12113. (c) Fonseca Guerra, C.; Bickelhaupt, F. M.; Snijders, J. G.; Baerends, E. J. *J. Am. Chem. Soc.* **2000**, *122*, 4117. (d) Deubel, D. V.; Sundermeyer, J.; Frenking, G. *J. Am. Chem. Soc.* **2000**, *122*, 10101. (e) Uddin, J.; Frenking, G. *J. Am. Chem. Soc.* **2001**, *123*, 1683. (f) Cedeño, D. L.; Weitz, E. *J. Am. Chem. Soc.* **2001**, *123*, 12857. (g) Bickelhaupt, F. M.; DeKock, R. L.; Baerends, E. J. *J. Am. Chem. Soc.* **2002**, *124*, 1500. (h) Baik, M.-H.; Friesner, R. A.; Lippard, S. J. *J. Am. Chem. Soc.* **2002**, *124*, 4495. (i) Deubel, D. V. *J. Am. Chem. Soc.* **2002**, *124*, 5834.
- (13) Frenking, G.; Fröhlich, N. *Chem. Rev.* **2000**, *100*, 717.
- (14) (a) Landis, C. R.; Cleveland, T.; Firman, T. K. *J. Am. Chem. Soc.* **1995**, *117*, 1859. (b) Landis, C. R.; Firman, T. K.; Root, D. M.; Cleveland, T. *J. Am. Chem. Soc.* **1998**, *120*, 1842. (c) Landis, C. R.; Cleveland, T.; Firman, T. K. *J. Am. Chem. Soc.* **1998**, *120*, 2641. (d) Firman, T. K.; Landis, C. R. *J. Am. Chem. Soc.* **1998**, *120*, 12650. (e) Firman, T. K.; Landis, C. R. *J. Am. Chem. Soc.* **2001**, *123*, 11728.
- (15) Bayse, C. A.; Hall, M. B. *J. Am. Chem. Soc.* **1999**, *121*, 1348.
- (16) Diefenbach, A.; Bickelhaupt, F. M.; Frenking, G. *J. Am. Chem. Soc.* **2000**, *122*, 6449.

- (17) Becke, A. D. *Phys. Rev. A* **1988**, *38*, 3098.
- (18) Lee, C.; Yang, W.; Parr, R. G. *Phys. Rev. B* **1988**, *37*, 785.
- (19) Van Lenthe, E.; Ehlers, A. E.; Baerends, E. J. *J. Chem. Phys.* **1999**, *110*, 8943 and refs cited therein.
- (20) (a) Fonseca Guerra, C.; Snijders, J. G.; Te Felde, G.; Baerends, E. J. *Theor. Chem. Acc.* **1998**, *99*, 391. (b) Bickelhaupt, F. M.; Baerends, E. J. In *Reviews in Computational Chemistry*; Lipkowitz, K. B., Boyd, D. B., Eds.; VCH: New York, 2000; Vol. 15, p 1. (c) Te Velde, G.; Bickelhaupt, F. M.; Baerends, E. J.; Fonseca Guerra, C.; Van Gisbergen, S. J. A.; Snijders, J. G.; Ziegler, T. *J. Comput. Chem.* **2001**, *22*, 931.

**Table 1.** Calculated Bond Distances (in Å) in  $P_4$  ( $T_d$ ) and  $Ag(P_4)_2^+$  ( $D_{2h}$  and  $D_{2d}$ )<sup>a</sup>

program	level of theory	$P_4$ P–P	$Ag(P_4)_2^+$							
			$D_{2h}$ (1)				$D_{2d}$ (2)			
			Ag–P1	P1–P2	P1–P3	P3–P4	Ag–P1	P1–P2	P1–P3	P3–P4
ADF	BLYP/V	2.218	2.563	2.389	2.206	2.250	2.564	2.383	2.205	2.251
G98	B3PW91/XXL	2.190	2.571	2.343	2.179	2.224	2.569	2.338	2.178	2.225
G98	MP2/XXL	2.197	2.492	2.380	2.189	2.231	2.483	2.373	2.189	2.233
	experiment	2.21 <sup>b</sup>	2.541 <sup>c</sup>	2.329 <sup>c</sup>	2.15 <sup>c</sup>	2.17 <sup>c</sup>				

<sup>a</sup> For more results, see Supporting Information. <sup>b</sup> Greenwood, N. N.; Earnshaw, A. *Chemistry of Elements*; Pergamon Press: Oxford, U.K., 1984. <sup>c</sup> Crossing, I. *Chem. Eur. J.* **2002**, *8*, 700.

**Table 2.** Calculated Stabilization Energy  $Ag^+ + 2 P_4 \rightarrow Ag(P_4)_2^+$  ( $\Delta E$ , in kcal/mol) for Each Conformer ( $D_{2h}$  and  $D_{2d}$ ) and Number  $n$  of Imaginary Frequencies<sup>a</sup>

program	level of theory	$D_{2h}$ (1)		$D_{2d}$ (2)	
		$\Delta E$	$n$	$\Delta E$	$n$
ADF	BLYP/V	−86.4		−86.3	
G98	B3PW91/XXL	−75.5 <sup>b</sup>	0	−75.5 <sup>c</sup>	0
G98	MP2/XXL	−82.7	0	−82.7	0

<sup>a</sup> For results at additional levels of theory, see Supporting Information. <sup>b</sup>  $\Delta S = -50.9$  cal/mol K,  $\Delta G = -57.9$  kcal/mol. <sup>c</sup>  $\Delta S = -49.4$  cal/mol K,  $\Delta G = -58.4$  kcal/mol.

**Table 3.** Energy Decomposition of the Ag– $P_4$  Bonds in the  $D_{2h}$  and  $D_{2d}$ -symmetric Conformers of  $Ag(P_4)_2^+$  at the BLYP/V Level<sup>a</sup>

contribution	$Ag(P_4)_2^+$	
	$D_{2h}$ (1)	$D_{2d}$ (2)
$\Delta E_{str}$	8.3	8.0
$\Delta E_{Pauli}$	148.3	147.5
$\Delta E_{elst}$	−127.1	−126.4
$\Delta E_{orb}$	−115.9	−115.4
$\Delta E_{orb}(\Gamma_i)$	<b><math>a_{1g}</math> (s, <math>d_{x^2-y^2}</math>, <math>d_{z^2}</math>) −56.9</b>	<b><math>a_1</math> (s, <math>d_{z^2}</math>) −55.5</b>
	<b><math>b_{1u}</math> (<math>p_z</math>) −18.0</b>	<b><math>e</math> (<math>p_x</math>, <math>p_y</math>, <math>d_{xz}</math>, <math>d_{yz}</math>) −37.2</b>
	<b><math>b_{2g}</math> (<math>d_{xz}</math>) −13.7</b>	<b><math>b_2</math> (<math>p_x</math>, <math>d_{xy}</math>) −18.9</b>
	<b><math>b_{3u}</math> (<math>p_x</math>) −13.6</b>	<b><math>b_1</math> (<math>d_{x^2-y^2}</math>) −2.5</b>
	<b><math>b_{2u}</math> (<math>p_y</math>) −5.1</b>	<b><math>a_2</math> (−) −1.5</b>
	<b><math>b_{3g}</math> (<math>d_{yz}</math>) −4.6</b>	
	<b><math>b_{1g}</math> (<math>d_{xy}</math>) −2.5</b>	
	<b><math>a_{1u}</math> (−) −1.5</b>	
$\Delta E_{int} = \Delta E_{Pauli} +$	−94.7	−94.3
$\Delta E_{elst} + \Delta E_{orb}$		
$\Delta E = \Delta E_{str} + \Delta E_{int}$	−86.4	−86.3

<sup>a</sup> Energies in kcal/mol. Bold: Contributions of the irreducible representations  $\Gamma_i$  to the stabilizing orbital-interaction energy  $\Delta E_{orb}$ ;  $\Gamma_i$ , metal orbitals involved (in parentheses), and energy  $\Delta E_{orb}(\Gamma_i)$  in kcal/mol.

−18.0 kcal/mol) and of the phosphorus lone pairs  $n(P)$  with  $5p_x$  ( $b_{3u}$ , −13.6 kcal/mol) are also significant (Figure 4). The MO diagram given in Figure 3 shows further details of the metal–ligand interactions: (i) an sd hybridization within  $a_{1g}$  symmetry, (ii) relatively small coefficients from vacant metal orbitals, and (iii) the additional involvement of occupied ligand orbitals in the metal–ligand interactions within  $b_{2g}$  orbital symmetry. The orbitals displayed in Figure 4 are the only orbitals that show significant changes in population upon the formation of the complex.

The strong participation of  $5p$  orbitals in metal–ligand bonding, which is clearly demonstrated by the energy contributions of the *ungerade* irreducible representations ( $b_{1u}$ ,  $b_{3u}$ ) to the stabilizing orbital interactions, is a remarkable result. The question whether  $np$  orbitals should be considered true valence

orbitals of transition metals has been the topic of a controversial discussion.<sup>13–16</sup> This question cannot be answered by using the standard version of the natural bond orbital analysis (NBO)<sup>22</sup> because of the a priori decision not to include the  $np$  functions in the valence space.<sup>23</sup> Firman et al.<sup>14</sup> suggested a valence-bond description of transition-metal complexes involving metal  $(n-1)d$  and  $ns$  orbitals only and validated their predicted structures of transition-metal hydrides by DFT calculations. In contrast, Bayse and Hall's<sup>15</sup> orbitally ranked symmetry analysis method (ORSAM) additionally considers  $np$  orbitals and therefore describes transition-metal complexes containing more than 12 valence electrons without introducing hypervalency. Diefenbach et al.<sup>16</sup> analyzed a series of isoelectronic third-row transition-metal carbonyl complexes and revealed a participation of  $6p$  orbitals. We now show that, in the  $P_4$  complex of silver(I), which is with its  $[Kr]4d^{10}$  configuration at the borderline of transition-metal and main-group elements, the energy contributions from ungerade symmetry to the stabilizing orbital interactions are as large as 32%.

The energy-decomposition analysis shown in Figure 4 reveals that there is an unexpectedly strong back-donation from the  $4d_{xz}$  orbital into the symmetry-adapted linear combination of vacant orbitals of the  $P_4$  cages ( $b_{2g}$ , −13.7 kcal/mol). Does this contribution determine the  $D_{2h}$  geometry of  $Ag(P_4)_2^+$ ? We have also calculated the structure and energy of the  $D_{2d}$ -symmetric conformer **2** (Figure 1). Surprisingly, the calculations predict the energies of both isomers **1** and **2** of  $Ag(P_4)_2^+$  to be equal (Table 3). The energy-decomposition analysis of **2** reveals that all contributions to the bond energy are very similar, unless identical with numerical accuracy, to the values of the  $D_{2h}$ -symmetric conformer **1** (Table 3). One might remark that the absence of a symmetry center in **2** prevents the  $4d_{xz}-\sigma^*$  interaction from being explicitly analyzed because the  $p_x$ ,  $p_y$ ,  $d_{xz}$ , and  $d_{yz}$  orbitals belong to the  $e$  irreducible representation (Table 3).<sup>5</sup> The contribution of  $e$  to the stabilizing orbital interactions in **2** is −38.3 kcal/mol, while the sum of the equivalent contributions ( $b_{3u} + b_{2u} + b_{2g} + b_{3g}$ ) in **1** is −38.2 kcal/mol. There is no evidence for an intrinsic stabilization of the  $D_{2h}$ -symmetric conformer by any of the contributions considered in our bond analysis. This conclusion is corroborated by virtually identical atomic charges<sup>24</sup> and bond distances in **1** and **2** (Figure 1).

Because the  $D_{2h}$  and  $D_{2d}$  isomers are isoenergetic and show equivalent bonding patterns, there is no preference for the  $D_{2h}$ -symmetric conformer by intramolecular interactions. A mainly electrostatic metal–ligand interaction would favor a tetrahedral

(21) The bond-energy contributions involving the  $5s$  orbital (vacant in  $Ag^+$ ) and the  $4d_{z^2}$  and  $4d_{x^2-y^2}$  orbitals (occupied in  $Ag^+$ ) cannot be analyzed separately because the three orbitals are totally symmetric (Table 3).

(22) Reed, A. E.; Curtiss, L. A.; Weinhold, F. *Chem. Rev.* **1988**, *88*, 899.

(23) Maseras, F.; Morokuma, K. *Chem. Phys. Lett.* **1992**, *195*, 500.

(24) Atomic charges in both **1** and **2** calculated using the Hirshfeld scheme (ref 25): Ag 0.24, P1 0.07, P3 0.12.

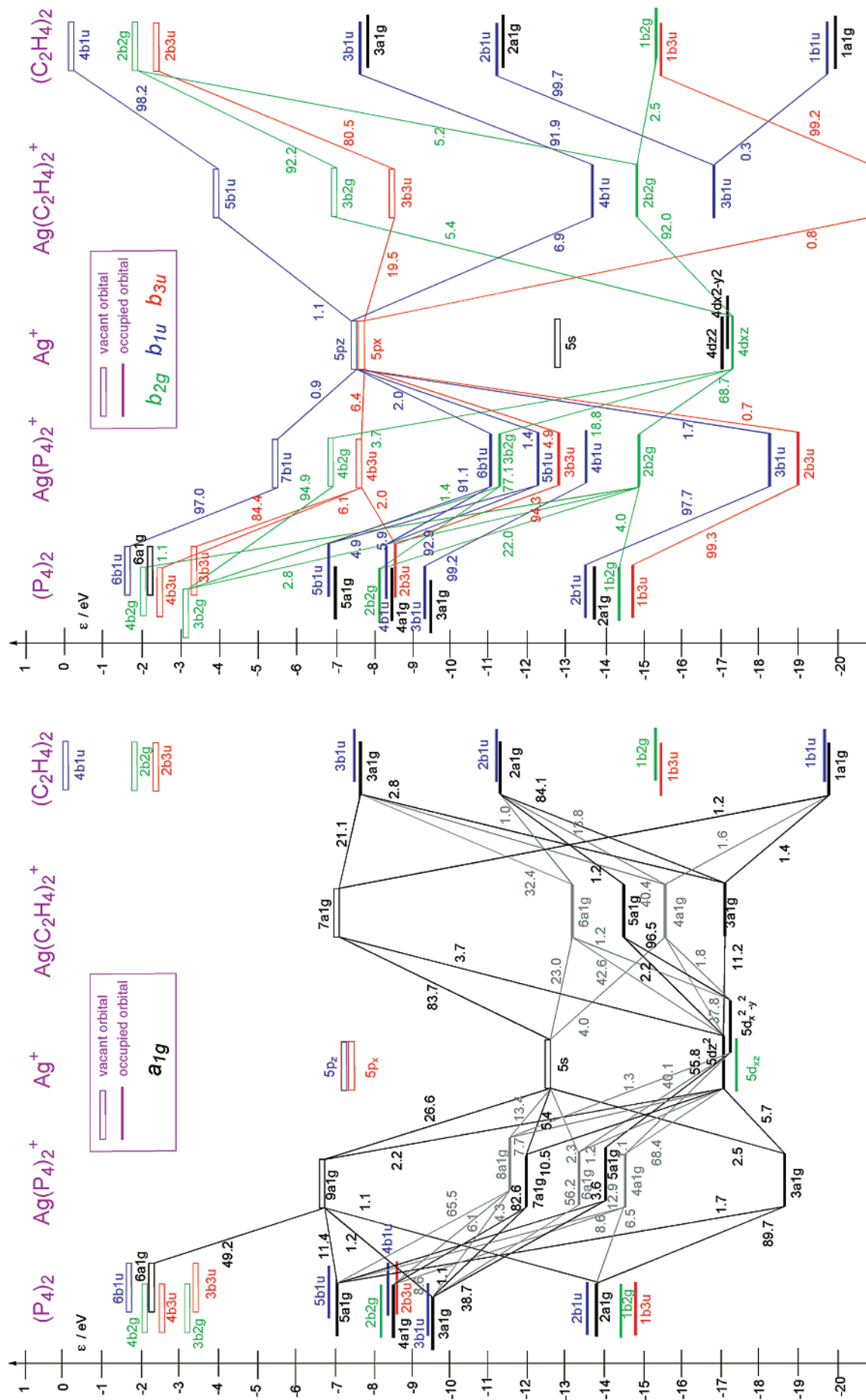


**Figure 3.** Comparative molecular orbital (MO) diagram of  $\text{Ag}(\text{P}_4)_2^+$  (1) and  $\text{Ag}(\text{C}_2\text{H}_4)_2^+$  (3) in  $D_{2h}$  symmetry. Expression of the molecular orbitals as a linear combination of metal orbitals and symmetry-adapted linear combinations (SALC) of ligand orbitals. Only interactions within  $\alpha_{ig}$  orbital symmetry (left) and  $b_{2g}$ ,  $b_{1u}$ , and  $b_{3u}$  orbital symmetry (right) are shown. Orbital energies  $\epsilon$  are given in eV, SALC contributions in percent. The orbitals that show significant changes in population upon the formation of the complexes are displayed in Figures 4 and 7.

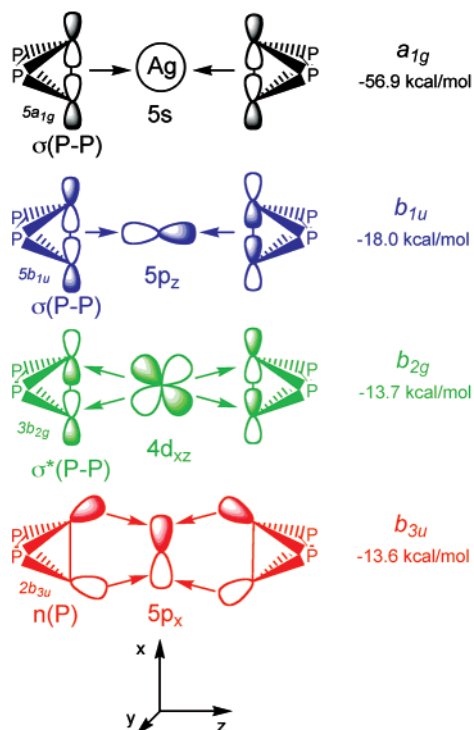


**Figure 4.** Main contributions of the irreducible representations to the stabilizing orbital-interaction energy  $\Delta E_{\text{orb}}$  in  $\text{Ag}(\eta^2\text{-P}_4)_2^+$  (**1**,  $D_{2h}$ ).

coordination environment;  $\text{Zn}^{2+}$  binding sites in zinc finger proteins are a typical example.<sup>26</sup> Since the ligands in  $\text{Ag}(\text{P}_4)_2^+$  are neutral, the electrostatic preference for the  $D_{2d}$  conformer is negligible. Orbital interactions do not induce a planar coordination environment; the analysis shows that there is essentially no difference between the involvement of one and two d orbitals in the  $\pi$ -type interaction with vacant orbitals of the pnictogene cages. The shallow rotational potential energy surface is also indicated by the fact that an isoenergetic  $D_2$ -symmetric isomer is predicted by calculations using a slightly smaller basis set (see Supporting Information). The  $D_{2h}$  structure observed experimentally is apparently induced by intermolecular interactions such as crystal packing and the polarizable environment which are difficult to consider by means of computational chemistry.<sup>27</sup>

### Comparison with $\text{Ag}(\text{C}_2\text{H}_4)_2^+$

Because the complexation of an olefin by a metal ion is an elementary reaction step in many industrial processes,<sup>29</sup> an understanding of the bonding in ethylene complexes is of fundamental interest.<sup>30–32</sup> We have also studied the bonding in

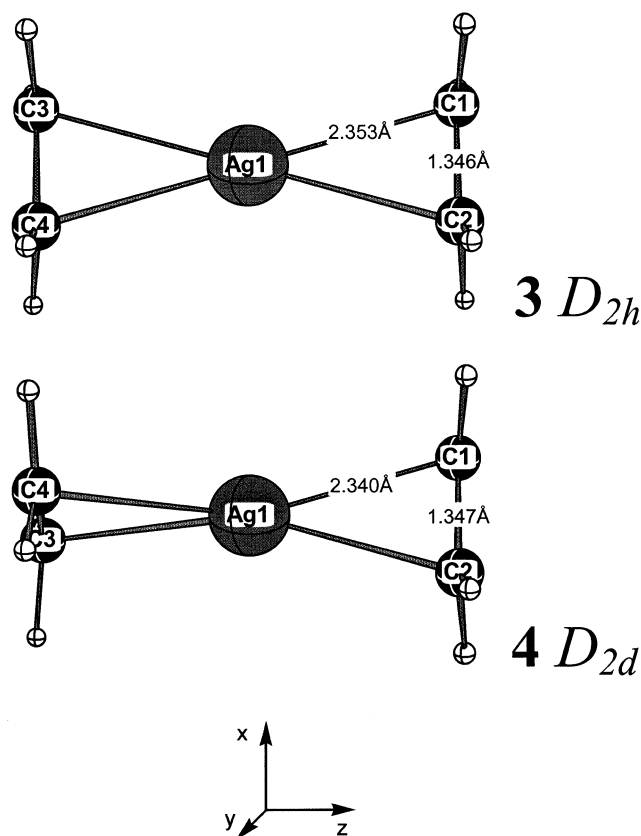


**Figure 5.** Calculated geometry (BLYP/V) of the conformers **3** and **4** of  $\text{Ag}(\text{C}_2\text{H}_4)_2^+$ .

**Table 4.** Calculated Bond Distances (in Å) in  $\text{C}_2\text{H}_4$  ( $D_{2h}$ ) and  $\text{Ag}(\text{C}_2\text{H}_4)_2^+$  ( $D_{2h}$  and  $D_{2d}$ )

program	level of theory	$\text{C}_2\text{H}_4$	$D_{2h}$ ( <b>3</b> )		$D_{2d}$ ( <b>4</b> )	
		C–C	Ag–C	C–C	Ag–C	C–C
ADF	BLYP/V	1.332	2.343	1.363	2.327	1.365
G98	B3PW91/XXL	1.324	2.351	1.354	2.340	1.355
G98	MP2/XXL	1.334	2.300	1.364	2.289	1.365

$\text{Ag}(\text{C}_2\text{H}_4)_2^+$  and compared to that in Krossing's cation. The calculated structures of the  $D_{2h}$  and  $D_{2d}$ -symmetric isomer (**3** and **4**) are displayed in Figure 5. Theoretically predicted bond distances and stabilization energies are listed in Tables 4 and 5. The metal–C distances (2.35 Å) are longer than those in late transition-metal ethylene complexes<sup>33</sup> and shorter than those in early transition-metal ethylene complexes.<sup>34</sup> Calculated stabilization enthalpies,  $\text{Ag}^+ + 2 \text{C}_2\text{H}_4 \rightarrow \text{Ag}(\text{C}_2\text{H}_4)_2^+$ , are in good agreement with the experimental value (Table 5). The metal–ligand energies are slightly smaller than in the *tetrahedro*- $\text{P}_4$  complexes and the  $D_{2d}$  structure **4** is found to be favored over the  $D_{2h}$ -symmetric conformer **3** by less than one kcal/mol (Table 5).<sup>35</sup>

- (25) Hirshfeld, E. L. *Theor. Chim. Acta* **1977**, *44*, 129.  
 (26) (a) Dudev, T.; Lim, C. J. *Phys. Chem. B* **2001**, *105*, 10709. (b) Dudev, T.; Lim, C. J. *Am. Chem. Soc.* **2002**, *124*, ja012620l-3–316, in press.  
 (27) Calculations employing microscopic models such as  $\text{CF}_4$  for the large spectator anions do not show a stabilization of the  $D_{2h}$  structure. Whether calculations using the conductor-like screening model (COSMO, ref 28) predict the two isomers to be isoenergetic or the  $D_{2h}$  structure to be preferred strongly depends on atomic radii used. Because of the lack of thermochemical data required for a parametrization, the definition of the molecular cavity is arbitrary.  
 (28) (a) Klamt, A.; Schürmann, G. *J. Chem. Soc., Perkin Trans. 2* **1993**, 799. (b) Klamt, A.; Jonas, V. *J. Chem. Phys.* **1996**, *105*, 9972.  
 (29) (a) *Advanced Inorganic Chemistry*, 6th edition; Cotton, F. A., Wilkinson, G., Murillo, C., Eds.; Wiley: New York, 1999. (b) *Catalysis from A to Z*; Cornils, B., Herrmann, W. A., Schlögl, R., Wong, C. H., Eds.; Wiley-VCH: Weinheim, Germany, 2000. (c) *Applied Homogeneous Catalysis with Organometallic Compounds*; Cornils, B., Herrmann, W. A., Eds.; Wiley-VCH: Weinheim, Germany, 2002.

- (30) Guo, B. C.; Castleman, A. W. *Chem. Phys. Lett.* **1991**, *181*, 16.  
 (31) Sievers, M. R.; Jarvis, L. M.; Armentrout, P. B. *J. Am. Chem. Soc.* **1998**, *120*, 1891.  
 (32) Quantum-chemical studies of  $\text{Ag}(\text{C}_2\text{H}_4)^+$ : refs 10, 30, and (a) Basch, H. *J. Chem. Phys.* **1972**, *56*, 441. (b) Ziegler, T.; Rauk, A. *Inorg. Chem.* **1979**, *18*, 1558. (c) Ma, N. L. *Chem. Phys. Lett.* **1998**, *297*, 230. (d) Schröder, D.; Wesendrup, R.; Hertwig, R. H.; Dargel, T. K.; Grauel, H. Koch, W.; Bender, B. R.; Schwarz, H. *Organometallics* **2000**, *19*, 2608. (e) Bouteau, L.; Leon, E.; Luna, A.; Toulhoat, P.; Tortajada, J. *Chem. Phys. Lett.* **2001**, *338*, 74.  
 (33) A typical  $\text{Pd}(\text{II})\text{-C}(\text{ethylene})$  distance is 2.15 Å; for instance, see: Deubel, D. V.; Ziegler, T. *Organometallics* **2002**, *21*, 1603.  
 (34) A typical  $\text{Mo}(\text{VI})\text{-C}(\text{ethylene})$  distance is 2.60 Å; for instance, see: Deubel, D. V.; Sundermeyer, J.; Frenking, G. *Inorg. Chem.* **2000**, *39*, 2314.

**Table 5.** Calculated Stabilization Energy  $\text{Ag}^+ + 2 \text{C}_2\text{H}_4 \rightarrow \text{Ag}(\text{C}_2\text{H}_4)_2^+$  ( $\Delta E$ , in kcal/mol) for Each Conformer ( $D_{2h}$  and  $D_{2d}$ ) and Number  $n$  of Imaginary Frequencies

program	level of theory	$D_{2h}$ (3)		$D_{2d}$ (4)	
		$\Delta E$	$n$	$\Delta E$	$n$
ADF	BLYP/V	-73.3		-73.8	
G98	B3PW91/XXL	-69.2 <sup>a</sup>	0	-69.7 <sup>b</sup>	0
G98	MP2/XXL	-69.6	0	-70.4	0
	experiment			-66.1 <sup>c</sup>	

<sup>a</sup>  $\Delta S = -51.7$  cal/mol K,  $\Delta G = -48.7$  kcal/mol. <sup>b</sup>  $\Delta S = -55.9$  cal/mol K,  $\Delta G = -47.8$  kcal/mol. <sup>c</sup> Guo, B. C.; Castleman, A. W., Jr. *Chem. Phys. Lett.* **1991**, *181*, 16.  $\Delta S = -52.3$  cal/mol K,  $\Delta G = -40.5$  kcal/mol. Experimental geometry not reported.

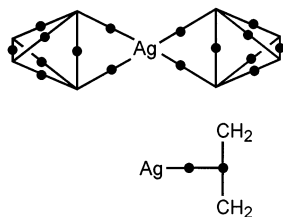


**Figure 6.** Topological analysis of electron density in  $\text{Ag}(\eta^2\text{-P}_4)_2^+$  and  $\text{Ag}(\text{C}_2\text{H}_4)_2^+$ . Bond paths (lines) and (3, -1) bond-critical points (dots) are shown. Is the T-shaped bonding pattern in the ethylene complex due to the absence of back-donation from the  $4d_{xz}$  orbital or due to a predominance of electrostatics?

Hertwig et al.<sup>10</sup> reported a topological analysis of electron density in  $\text{Ag}(\text{C}_2\text{H}_4)_2^+$  using Bader's atoms in molecules (AIM)<sup>9</sup> concept. The AIM method provides an aesthetic and well-defined description of the chemical bond.<sup>13</sup> For instance, (3,-1) bond-critical points correspond to a minimum of electron density in the direction of a bond and to maximums of electron density in the perpendicular directions of space, indicating the center of a chemical bond. Krossing and Van Wüllen<sup>6</sup> recently reported an AIM analysis of the  $\text{Ag}(\text{P}_4)_2^+$  complex and found bond-critical points (i) between all P atoms and (ii) between the metal and the phosphorus atoms coordinating with the metal ( $\Delta$ -shaped bonding pattern). This is shown in Figure 6. In contrast, the analysis of the ethylene complex<sup>10</sup> shows a T-shaped bonding pattern with bond-critical points (i) between the carbon atoms and (ii) *between this bond-critical point and the metal*. (Figure 5).<sup>10,36</sup> It was suggested that the  $\text{Ag}^+ - \text{C}_2\text{H}_4$  bond is mainly electrostatic in origin and there is little or no back-bonding from the occupied  $4d$  orbitals of  $\text{Ag}^+$  to the ethylene ligand, in contrast to the bonding in Krossing's cation, indicating a fundamentally different metal–ligand interaction in olefin and  $\eta^2\text{-P}_4$  complexes.<sup>6,10</sup>

The results of the analysis of  $\text{Ag}(\text{C}_2\text{H}_4)_2^+$  (3,  $D_{2h}$ ) are presented in Table 6 and Figure 7. The interaction energy  $\Delta E_{\text{int}}$  (-76.8 kcal/mol) calculated at the BLYP level is smaller than that in  $\text{Ag}(\text{P}_4)_2^+$  (-94.7 kcal/mol), so are its three components ( $\Delta E_{\text{Pauli}}$ ,  $\Delta E_{\text{elst}}$ , and  $\Delta E_{\text{orb}}$ ). Given the puzzling AIM results in Figure 5, it is remarkable to note the very similar energy contributions in the complexes with the two ligands. The bond-energy contributions in  $\text{Ag}(\text{P}_4)_2^+$  and  $\text{Ag}(\text{C}_2\text{H}_4)_2^+$  essentially match, including the ratio of electrostatics and stabilizing orbital interactions on one hand and the partitioning of the latter term

(35) Atomic charges in both 3 and 4 calculated using the Hirshfeld scheme (ref 25): Ag 0.46, C -0.02, H 0.08. In ethylene: C -0.08, H 0.04.

(36) The presence of bond-critical points can depend on method. Compare ref 10 with Böhme, C.; Wagener, T.; Frenking, G. *J. Organomet. Chem.* **1996**, *520*, 31.

**Table 6.** Energy Decomposition of the  $\text{Ag}-\text{C}_2\text{H}_4$  Bonds in the  $D_{2h}$  and  $D_{2d}$ -symmetric Conformers of  $\text{Ag}(\text{C}_2\text{H}_4)_2^+$  at the BLYP/V Level<sup>a</sup>

contribution	$\text{Ag}(\text{C}_2\text{H}_4)_2^+$	
	$D_{2h}$	$D_{2d}$
$\Delta E_{\text{str}}$	3.5	3.8
$\Delta E_{\text{Pauli}}$	108.2	113.6
$\Delta E_{\text{elst}}$	-103.6	-107.4
$\Delta E_{\text{orb}}$	-81.4	-83.6
$\Delta E_{\text{orb}}(\Gamma_i)$	<b><math>a_{1g}</math> (s, <math>d_{x^2-y^2}</math>, <math>d_{z^2}</math>) -45.4</b>	<b><math>a_1</math> (s, <math>d_{z^2}</math>) -45.5</b>
	<b><math>b_{1u}</math> (<math>p_z</math>) -13.5</b>	<b><math>e</math> (<math>p_x</math>, <math>p_y</math>, <math>d_{xz}</math>, <math>d_{yz}</math>) -21.4</b>
	<b><math>b_{2g}</math> (<math>d_{xz}</math>) -12.5</b>	<b><math>b_2</math> (<math>p_z</math>, <math>d_{xy}</math>) -14.0</b>
	<b><math>b_{3u}</math> (<math>p_x</math>) -2.5</b>	<b><math>b_1</math> (<math>d_{x^2-y^2}</math>) -1.4</b>
	<b><math>b_{2u}</math> (<math>p_y</math>) -2.3</b>	<b><math>a_2</math> (-) -1.3</b>
	<b><math>b_{3g}</math> (<math>d_{yz}</math>) -2.6</b>	
	<b><math>b_{1g}</math> (<math>d_{xy}</math>) -1.3</b>	
	<b><math>a_{1u}</math> (-) -1.1</b>	
$\Delta E_{\text{int}} = \Delta E_{\text{Pauli}} + \Delta E_{\text{elst}} + \Delta E_{\text{orb}}$	-76.8	-77.6
$\Delta E = \Delta E_{\text{str}} + \Delta E_{\text{int}}$	-73.3	-73.8

<sup>a</sup> Energies in kcal/mol. Bold: Contributions of the irreducible representations  $\Gamma_i$  to the stabilizing orbital-interaction energy  $\Delta E_{\text{orb}}$ ;  $\Gamma_i$ , metal orbitals involved (in parentheses), and energy  $\Delta E_{\text{orb}}(\Gamma_i)$  in kcal/mol.

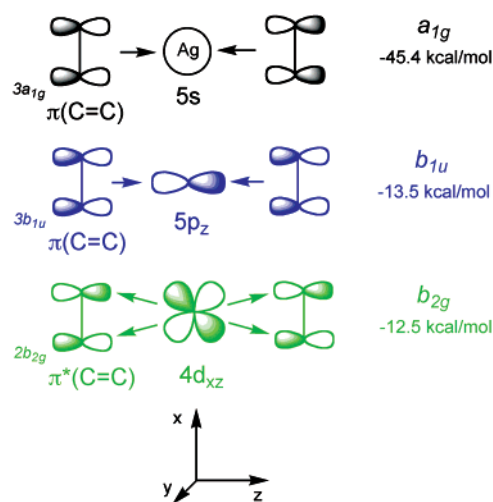


**Figure 7.** Main contributions of the irreducible representations to the stabilizing orbital-interaction energy  $\Delta E_{\text{orb}}$  in  $\text{Ag}(\text{C}_2\text{H}_4)_2^+$  (3,  $D_{2h}$ ).

into the irreducible representations on the other hand (Tables 3 and 6).<sup>37</sup> Surprisingly, back-donation from the silver  $d_{xz}$  orbital to vacant orbitals of the olefins ( $b_{2g}$ ) is found to provide an even larger relative contribution to the orbital-interaction energy than the corresponding contribution in the  $\text{P}_4$  complex, despite the T-shaped bond paths in the ethylene complex and the  $\Delta$ -shaped bond paths in the  $\text{P}_4$  complex. However, we identify one *qualitative* difference between the two silver complexes: The  $b_{3u}$  contribution is as large as -13 kcal/mol in  $\text{Ag}(\text{P}_4)_2^+$  but essentially missing in  $\text{Ag}(\text{C}_2\text{H}_4)_2^+$ . This is simply caused by the fact that an occupied  $b_{3u}$  symmetry-adapted linear combination (SALC) of the ethylene's frontier orbitals is not available.

*Quantitative* differences between the two complexes can be summarized as follows. (i) The contributions from  $a_{1g}$  and  $b_{1u}$  are larger in the  $\text{P}_4$  complex than in the  $\text{C}_2\text{H}_4$  complex, possibly because the orbital energy levels of the phosphorus cages are higher than the  $\pi$ -orbital energy of the C=C bond (Table 7,

(37) An energy-decomposition analysis of  $\text{Ag}(\text{C}_2\text{H}_4)_2^+$  does not provide insight into the contributions from  $4d$ ,  $5s$ , and  $5p$  orbitals to the bond energy because the complex is  $C_{2v}$ -symmetric (ref 10).

**Table 7.** Frontier-Orbital Energies  $\epsilon$  (in eV) of  $\text{Ag}^+$  and of the Symmetry-Adapted Linear Combinations (SALC) of  $(\text{P}_4)_2$  and  $(\text{C}_2\text{H}_4)_2$ , Respectively. Overlap Integrals between the  $\text{Ag}^+$  Orbital and SALC for Each Irreducible Representation  $\Gamma_i$

orbital	silver		ligands			overlap	
	$\epsilon$	$\Gamma_i$	$\epsilon(\text{P}_4)_2$	$\epsilon(\text{C}_2\text{H}_4)_2$	$\text{Ag}(\text{P}_4)_2^+$	$\text{Ag}(\text{C}_2\text{H}_4)_2^+$	
5s	-12.5	$a_{1g}$	-7.0	-7.6	0.39	0.43	
5p <sub>z</sub>	-7.2	$b_{1u}$	-6.8	-7.4	0.39	0.44	
5p <sub>x</sub>	-7.2	$b_{3u}$	-8.4	-15.4	0.43	0.30	
4d <sub>xz</sub>	-17.0	$b_{2g}$	-3.2	-1.9	0.12	0.18	

Figures 3 and 4). (ii) The contributions from  $b_{2g}$  in the  $\text{P}_4$  and  $\text{C}_2\text{H}_4$  complexes are equal, although the energy of the  $\sigma^*(\text{P}-\text{P})$  orbital is lower than the energy of the  $\pi^*(\text{C}=\text{C})$  orbital. The greater  $\langle 4d_{xz} | \pi^*(\text{C}=\text{C}) \rangle$  overlap integral in comparison with the  $\langle 4d_{xz} | \sigma^*(\text{P}-\text{P}) \rangle$  overlap integral apparently compensates for the frontier-orbital energy differences (Table 7, Figures 3 and 4), making the energy contributions of  $b_{2g}$  in both complexes equal.

The analysis reveals that the origin of the different topology of electron density in Krossing's cation and its ethylene counterpart is neither a predominance of electrostatics in  $\text{Ag}(\text{C}_2\text{H}_4)_2^+$  nor the absence of electron back-donation from the  $4d^{10}$  closed-shell to the ethylene ligands ( $b_{2g}$ ). The lack of an occupied symmetry-adapted linear combination of the ligand's frontier orbitals that can interact with the  $5p_x$  orbital of silver ( $b_{3u}$ ) causes the significantly different bonding patterns within the atoms-in-molecules framework. This quantum-chemical study highlights the use of orbital symmetry for understanding chemistry,<sup>47</sup> which was particularly demonstrated by the prediction of reactivity and stereoselectivity in pericyclic reactions.<sup>48</sup>

## Computational Methods

Geometry optimizations and energy calculations were performed at the gradient-corrected density functional theory (DFT) level using Becke's exchange functional<sup>17</sup> and Lee et al.'s correlation functional<sup>18</sup> (BLYP) as implemented in the Amsterdam Density Functional 2000 program, (ADF).<sup>20</sup> Relativistic effects were considered by the zero-order regular approximation (ZORA).<sup>19</sup> Uncontracted Slater-type orbitals (STOs) were used as basis functions.<sup>38</sup> The valence basis functions at Ag have triple- $\zeta$  quality, augmented with a set of p and f functions. The valence basis set at the other atoms has triple- $\zeta$  quality, augmented with a set of d and f functions. The  $(1s)^2$  core electrons of C, the  $(1s2s2p)^{10}$  core electrons of P, and the  $(1s2s2p3s3p3d)^{28}$  core electrons of Ag were treated within the frozen-core approximation.<sup>39</sup> This basis-set combination is denoted V. Geometry optimizations and energy calculations were also carried out using Becke's DFT-Hartree-Fock

hybrid method<sup>40</sup> which includes Perdew and Wang's correlation functional<sup>41</sup>(B3PW91)<sup>42</sup> as implemented in Gaussian 98 (G98).<sup>43</sup> An energy-consistent scalar-relativistic small-core effective core potential (ECP)<sup>44</sup> with the corresponding basis set fully decontracted and augmented with a set of f functions<sup>45</sup> was employed for the silver atom, while the basis sets 6-311+G(3df) and 6-311+G(2d,p) were used at phosphorus and at the other atoms, respectively. This basis-set combination is denoted XXL. Ab initio calculations at the Møller-Plesset second-order perturbation theory (MP2) level<sup>46</sup> were also performed with basis set XXL. The stationary points calculated with G98 were characterized by the number  $n$  of imaginary frequencies. Unscaled vibrational frequencies were considered in a thermochemical analysis. Additional calculations were carried out at various levels of theory using the ADF and G98 programs (see Supporting Information). For the analysis of the metal-ligand bonds, Ziegler and Rauk's<sup>11-13</sup> energy decomposition scheme was employed.

**Acknowledgment.** The author thanks Ingo Krossing, Timothy K. Firman, Aida H. Tai, Tom Ziegler, and the referees for helpful comments. He gratefully acknowledges support from, Carmay Lim, Alexander M. Mebel, and Michele Parrinello. The author also thanks the Federal Ministry of Education and Research, Germany (BMBF), and the Fonds der Chemischen Industrie for a Liebig Fellowship and the Alexander-von-Humboldt Foundation for a Feodor-Lynen Fellowship.

**Supporting Information Available:** Structures, energies, and energy decomposition of  $\text{Ag}(\text{P}_4)_2^+$  calculated at various levels of theory (PDF). This material is available free of charge via the Internet at <http://pubs.acs.org>.

JA0206691

- (40) Becke, A. D. *J. Chem. Phys.* **1993**, *98*, 5648.  
 (41) Perdew, J. P.; Wang, Y. *Phys. Rev.* **1992**, *B45*, 13244.  
 (42) The B3PW91 functional was successfully used for the investigation of phosphorous compounds: Cotton, F. A.; Cowley, A. H.; Feng, X. *J. Am. Chem. Soc.* **1998**, *120*, 1795.  
 (43) Frisch, M. J.; Trucks, G. W.; Schlegel, H. B.; Scuseria, G. E.; Robb, M. A.; Cheeseman, J. R.; Zakrzewski, V. G.; Montgomery, J. A.; Stratmann, R. E.; Burant, J. C.; Dapprich, S.; Milliam, J. M.; Daniels, A. D.; Kudin, K. N.; Strain, M. C.; Farkas, O.; Tomasi, J.; Barone, V.; Cossi, M.; Cammi, R.; Mennucci, B.; Pomelli, C.; Adamo, C.; Clifford, S.; Ochterski, J.; Petersson, G. A.; Ayala, P. Y.; Cui, Q.; Morokuma, K.; Malick, D. K.; Rabuck, A. D.; Raghavachari, K.; Foresman, J. B.; Cioslowski, J.; Ortiz, J. V.; Stefanov, B. B.; Liu, G.; Liashenko, A.; Piskorz, P.; Komaromi, I.; Gomberts, R.; Martin, R. L.; Fox, D. J.; Keith, T. A.; Al-Laham, M. A.; Peng, C. Y.; Nanayakkara, A.; Gonzalez, C.; Challacombe, M.; Gill, P. M. W.; Johnson, B. G.; Chen, W.; Wong, M. W.; Andres, J. L.; Head-Gordon, M.; Replogle, E. S.; Pople, J. A. *Gaussian98*; Gaussian Inc.: Pittsburgh, PA, 1998.  
 (44) Dolg, M.; Stoll, H.; Preuss, H.; R. M. Pitzer, R. M. *J. Phys. Chem.* **1993**, *97*, 5852.  
 (45) Ehlers, A. W.; Böhme, M.; Dapprich, S.; Gobbi, A.; Höllwarth, A.; Jonas, V.; Köhler, K. F.; Stegmann, R.; Veldkamp A.; Frenking, G. *Chem. Phys. Lett.* **1993**, *208*, 111.  
 (46) Møller, C.; Plesset, M. S. *Phys. Rev.* **1934**, *46*, 618.  
 (47) Simmons, H. E., Bunnett, J. F., Eds. *Orbital Symmetry Papers*; American Chemical Society: Washington, DC, 1974.  
 (48) (a) Hoffmann, R.; Woodward, R. B. *Science* **1970**, *167*, 825. (b) Houk, K. N.; Gonzalez, J.; Li, Y. *Acc. Chem. Res.* **1995**, *28*, 81.

(38) Snijders, J. G.; Baerends, E. J.; Vernooijs, P. *At. Data Nucl. Data Tables* **1982**, *26*, 483.

(39) Baerends, E. J.; Ellis, D. E.; Ros, P. *Chem. Phys.* **1973**, *2*, 41.